

**NANO COMMENTARY**

**Open Access**

# Characterization of hybrid cobalt-porous silicon systems: protective effect of the Matrix in the metal oxidation

Álvaro Muñoz-Noval<sup>1,2</sup>, Darío Gallach<sup>1</sup>, Miguel Ángel García<sup>2,3</sup>, Vicente Ferro-Llanos<sup>4</sup>, Pilar Herrero<sup>5</sup>, Kazuhiro Fukami<sup>6</sup>, Yukio H Ogata<sup>6</sup>, Vicente Torres-Costa<sup>1</sup>, Raúl J Martín-Palma<sup>1\*</sup>, Aurelio Ciment-Font<sup>1</sup> and Miguel Manso-Silván<sup>1</sup>

## Abstract

In the present work, the characterization of cobalt-porous silicon (Co-PSi) hybrid systems is performed by a combination of magnetic, spectroscopic, and structural techniques. The Co-PSi structures are composed by a columnar matrix of PSi with Co nanoparticles embedded inside, as determined by Transmission Electron Microscopy (TEM). The oxidation state, crystalline structure, and magnetic behavior are determined by X-Ray Absorption Spectroscopy (XAS) and Alternating Gradient Field Magnetometry (AGFM). Additionally, the Co concentration profile inside the matrix has been studied by Rutherford Backscattering Spectroscopy (RBS). It is concluded that the PSi matrix can be tailored to provide the Co nanoparticles with extra protection against oxidation.

**Keywords:** Porous silicon, Hybrid materials, Metal electroinfiltration, Transmission electron microscopy

## Background

The development of hybrid materials is a current topic of research with many potential applications in several fields, including optoelectronics, catalysis, and biomedicine. Concretely, the hybridization of semiconductors with ferromagnetic material such as cobalt, iron, and nickel gives the possibility to obtain materials that combine semiconducting and magnetic properties [1]. Moreover, the continuous progress in nanotechnology during the last decades has led to a large availability of techniques for the fabrication and characterization of nanometric structures with controlled composition and dimensions, resulting in nanostructures with very specific properties and several functionalities [2]. In fact, multifunctional metal-based nanostructures have received a great deal of attention during the past few years given their special properties and potential applications in many scientific and technologic fields, including biomedicine [3]. In this sense, the conjugation of magnetic-semiconductor hybrid nanosystems has allowed manipulation of local spin in

spintronics [4,5] and the fabrication of high sensitive magnetic sensors [6]. Regarding porous semiconductors such as porous silicon (PSi), they present additional advantages including high surface area and high surface reactivity [7].

This work aims at studying the oxidation state and crystalline structure of cobalt nanoparticles (NPs) embedded into porous silicon, resulting in Co-PSi hybrid structures. Co has been infiltrated into the PSi matrix by electrochemical techniques [8]. The suitability of PSi to host Co NPs grown by electroinfiltration has been evaluated, and both the magnetic and structural properties of the hybrid structures have been studied. The role of the porous matrix protecting Co against oxidation has been evaluated by infiltrating the Co NPs into PSi layers with different morphologies. The chemical and structural states of the Co NPs have been determined by combining highly selective and sensitive characterization techniques such as X-Ray Absorption Spectroscopy-synchrotron (XAS-synchrotron) and Rutherford Backscattering (RBS).

## Methods

### Preparation of porous silicon

Porous silicon (PSi), both as single layers and multilayers, was obtained from high conductivity (0.01-0.02

\* Correspondence: rajulose.martin@uam.es

<sup>1</sup>Departamento de Física Aplicada, Universidad Autónoma de Madrid, Cantoblanco, Madrid 28049, Spain

Full list of author information is available at the end of the article

$\Omega\text{cm}$ ), p-type, silicon wafers. The anodization in 1:2 (volume) HF:ethanol solutions (from commercial HF 48% (w/v) in water, Sigma-Aldrich) was carried out in a homemade Teflon<sup>®</sup> electrochemical cell, with a Pt reference electrode. The Si wafers were galvanostatically etched under illumination from a 100 W halogen lamp. Single layer PSi were obtained at  $100\text{ mA/cm}^2$  for 100 s, resulting in layers of about 10 microns. Different current densities were set for obtain different porosities from 40 to  $120\text{ mA/cm}^2$  in case of multilayer configurations (Figure 1). Two different porosity gradients were chosen to electrochemically grow Co NPs into PSi: A negative gradient (more porous towards the surface) and a positive gradient (more porous towards the substrate). In both cases the current densities applied were in four steps: 20, 40, 60 and  $80\text{ mA/cm}^2$ . After etching, the Si/PSi substrates were rinsed in ethanol and dried with  $\text{N}_2$ .

#### Electroinfiltration of Co

Electroinfiltration of Co nanoparticles into PSi single- and multi-layers was carried out in a electrochemical bath with a Watt's solution at RT ( $\text{CoSO}_4 \cdot 7\text{H}_2\text{O}$  0.2 M,  $\text{CoCl}_2$  0.05,  $\text{H}_3\text{BO}_3$  0.4 M, Na-Saccharine 25 g/l  $\text{H}_2\text{SO}_4$  1 mM). Boric acid was used as a buffer, to avoid pH fluctuations, sodic saccharine as crystallization catalyzer and sulfuric acid to decrease the pH of the solutions below 3. A well parameterized pulsed current process was used to allow the nucleation of metal nanoparticles into the pores of pulses of  $40\text{ mA/cm}^2$  and 10 s. An important parameter in pulsed mode is the equilibrium time or rest time, between pulses, set at 60 s; estimated by observing the dynamics of the voltage versus time curves (not shown). A overall view of the whole process of PSi single/multi layer fabrication and Co electroinfiltration is summarized in Figure 2.

#### Characterization

**Field emission scanning electron microscopy (FESEM)** images were obtained in a XL 30S-FEG (PHILIPS). No metallization was required to observe the samples. Samples for cross section observation were prepared according to previously optimized protocols for mechanical and ion bean milling [9]. TEM/STEM characterization was carried

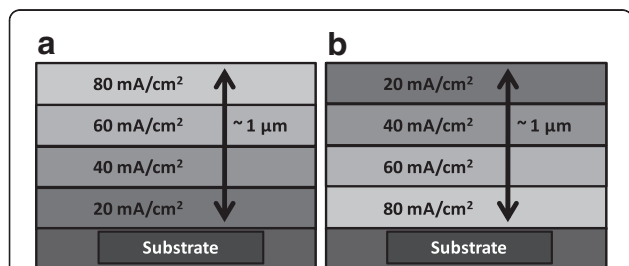


**Figure 1** Scheme of the configuration of the PSi multilayers used for XAS experiments: (a) negative gradient configuration, Co-PSi-n; (b) positive gradient configuration, Co-PSi-p.

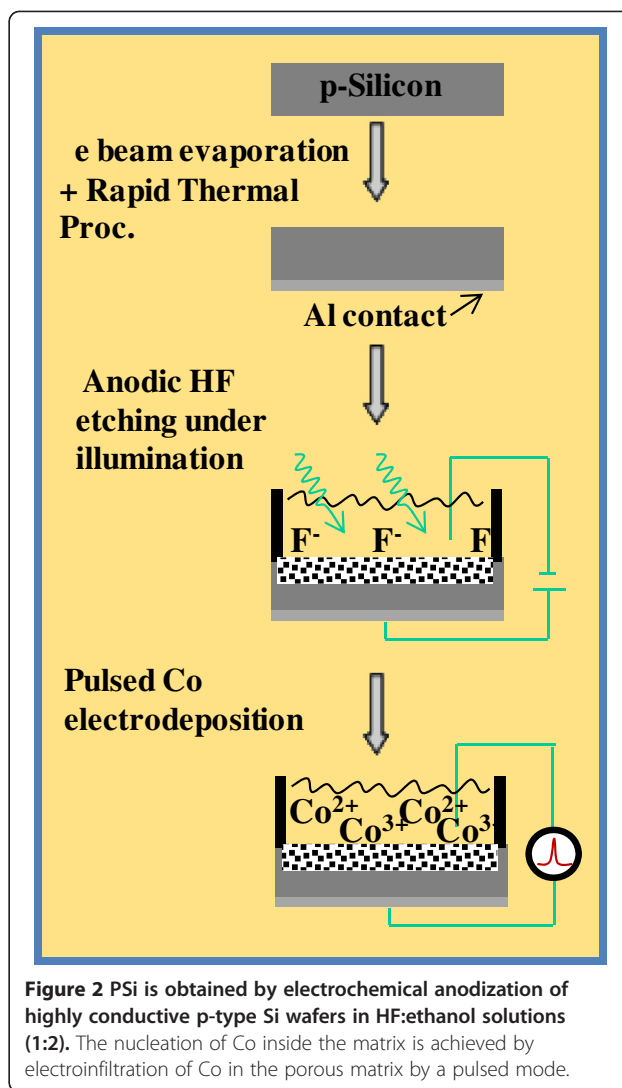


**Figure 2** PSi is obtained by electrochemical anodization of highly conductive p-type Si wafers in HF:ethanol solutions (1:2). The nucleation of Co inside the matrix is achieved by electroinfiltration of Co in the porous matrix by a pulsed mode.

out using a Jeol JEM 3000F with HAADF (High Angle Annular Dark Field) system included (300kV).

#### X-ray Absorption Spectroscopy (XAS)

X-Ray Absorption Near-Edge Structure (XANES) and Extended X-ray Absorption Fine Structure (EXAFS) spectroscopy measurements at the Co K-edge energy (7704.9 eV) were performed at room temperature in fluorescence mode at the BM25 Spanish CRG Beamline (SpLine) of the ESRF (European Synchrotron Radiation Facility). An INCA 13 elements X-Ray detector was used. Bulk metallic Co, plus  $\text{CoO}$  and  $\text{Co}_3\text{O}_4$  powders were measured as references. Data were normalized applying the same normalization parameters for all the spectra by means of Athena Software [10].

#### Alternating gradient field magnetometry

Magnetic characterization was performed using a Micro-mag Model 2900 Alternating Gradient Magnetometer

System (Princeton Measurements Corporation). Nine measurements were taken for each sample. Measurements were carried out applying a magnetic field from -100mT to 100mT, a time pass of 100 ms, and a field pass of 800 $\mu$ T.

#### Rutherford backscattering spectroscopy

Micro analytical techniques were used to obtain in-depth elemental information. A Cockcroft-Walton tandem accelerator located at Centro de Micro-Análisis de Materiales (CMAM, Universidad Autónoma de Madrid, Spain) was used for Rutherford Backscattering Spectroscopy (RBS). RBS was performed with a 3.050 MeV He<sup>+</sup> beam (incidence angle was 75° with respect to the surface normal). RBS was acquired by using silicon surface barrier detectors placed at scattering angle of 170°. A 13  $\mu$ m thick mylar foil was placed in front of the detector on the forward scattering angle to stop the He forward scattered particles and filter the H recoils. All RBS experiments were performed in vacuum (pressure lower than 10E-5 mbar). All spectra were simulated using the SIMNRA code [11] to obtain the element in-depth composition.

## Results and discussion

### PSi single layers

Preliminary structural studies of Co-PSi hybrid structures are carried out by Transmission Electron Microscopy (TEM) in a milled sample of single layer Co-PSi. As Figure 3 shows, Co ions infiltrate inside the PSi matrix and form spherical nanoparticles (NP) into the pores. In this case, nanoparticles of circa 5 nm are formed. Scanning TEM (STEM) images plus EDX analysis of these Systems (Figure 3) allow the identification of both elements in the NP.

Magnetic properties of single layer PSi-Co are evaluated by Alternating Gradient Field Magnetometry (AGFM). Samples electroinfiltrated at an increasing number of cycles with Co, from 5 to 20 cycles, are evaluated. Saturation magnetization values normalized to mass increase with increasing number of cycles in the studied range of cycles. Results point to the possibility of tailoring the magnetization of Co-PSi by controlling the amount of Co inside the PSi matrix (Figure 4). This is

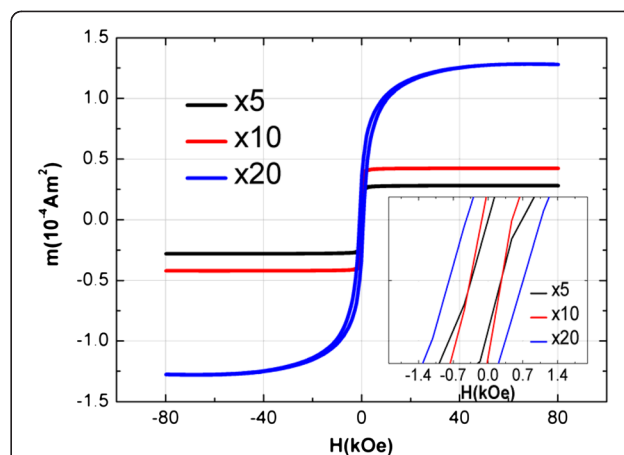


**Figure 4** AGFM magnetization curve for Co-PSi systems with increasing Co concentration inside the matrix, obtained from increasing number of electroinfiltration pulses: 5, 10 and 20. Demonstrating the control of the matrix filling with Co. (inset) Axis detail showing coercivity dependence of the magnetic material for increasing amount of internalized Co nanoparticles.

achieved by setting the number of electroinfiltration pulses during the synthesis process. Coercivity magnitude of the material depends on the amount of Co in the hybrid material: less concentrated systems present lower coercivity values [4,6]; systems with higher Co concentration present higher values. This feature can be due to the appearance of inter-particle correlations inside the matrix or by the increase of the size of particles [12] favoured by an increasing density of NPs into the PSi matrix.

### PSi multilayers

Once studied the magnetic potential of Co-PSi systems, the protective effect of the PSi matrix against the oxidation of Co is determined. Magnetic properties of Co strongly depend on the oxidation state and therefore determine the possible applications of these hybrid systems [13]. For this purpose a multilayer PSi is fabricated and infiltrated with Co. Two multilayer configurations are made, as Figure 1 shows, one with a negative porosity gradient (Co-PSi-n) and other with a positive one (Co-PSi-p). These systems are studied by XAS [14-16] (Figure 5).

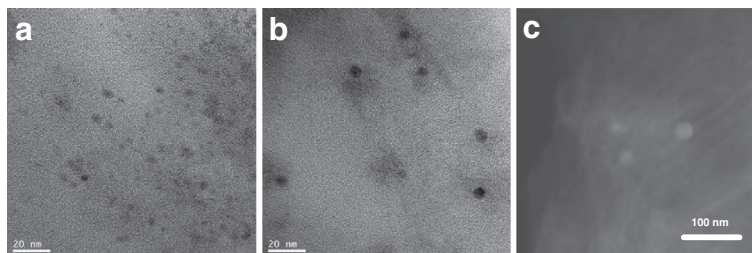


**Figure 3** (a,b) TEM images of typical Co-PSi structures showing Co NPs into the PSi matrix; (c) STEM image of typical Co-PSi structures, showing the Co NPs in a brighter tone than the matrix, composed by a lighter element (Si and O).

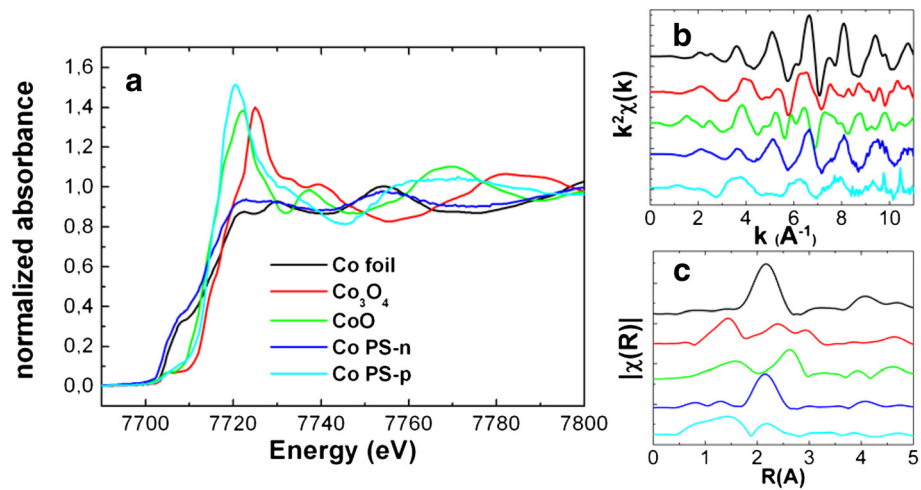


**Figure 5** XAS spectra of the Co references and Co-PSi multilayer systems: a) XANES spectra, b) EXAFS spectra of the references and samples; c) Radial Distribution Functions of the referred samples.

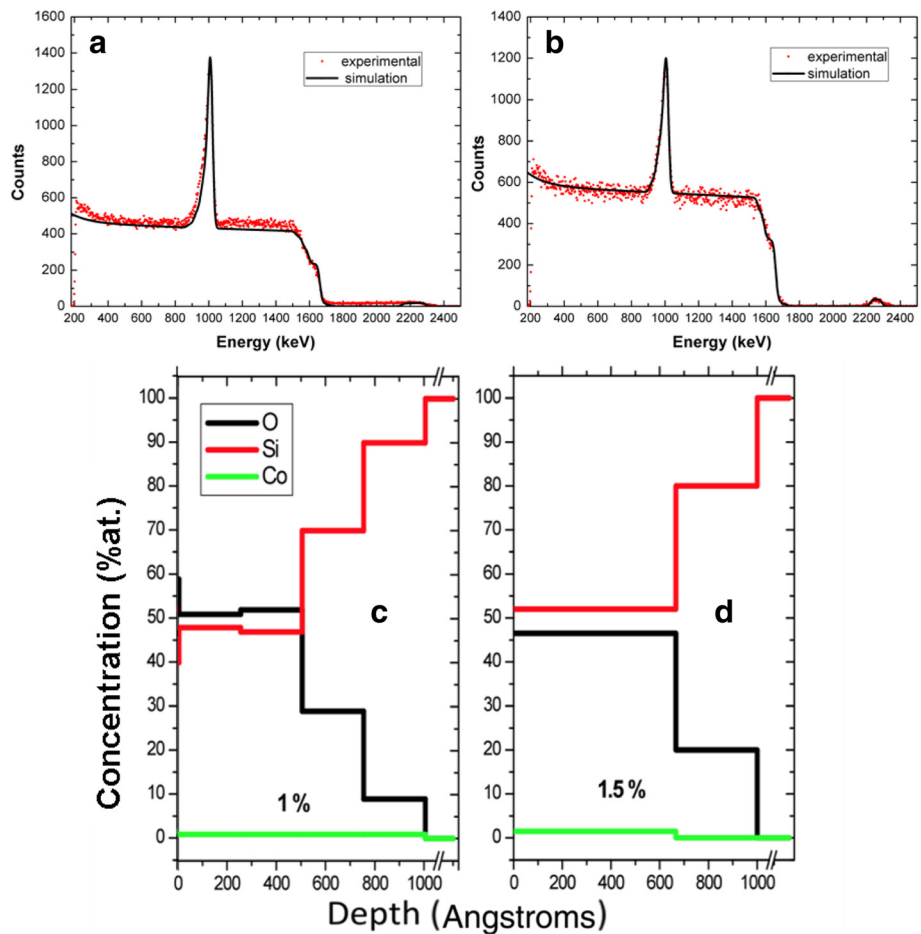


**Figure 6** (a,b) RBS spectra of Co-PSi-n and Co-PSi-p systems, respectively showing experimental data (dots), and simulation (lines). (c and d) Elemental concentration profiles of Co-PSi-n and Co-PSi-p, respectively obtained from simulations of the spectra shown in a and b.



XANES spectra (Figure 5a) of both systems show clear differences in oxidation state. Co and Cobalt oxides references are obtained for comparing and adjusting the experimental spectra to known materials. From the fitting of the experimental data to references it can be observed that in Co-PSi-n systems, Co atoms are mainly in metallic state (close to 90% at.) and the remaining 10% at. is in the form  $\text{Co}_3\text{O}_4$ . Besides, studying Co-PSi systems shows Co to be composed by a mix of Co (40%at.), CoO (50%at.) and  $\text{Co}_3\text{O}_4$  (10%at). The EXAFS spectra of the Co-PSi show the element environment and lattice structure in the Fourier space (Figure 5b). Comparing the EXAFS spectra of the Co-PSi systems with the reference it is straightforward to identify similarities of that of Co-PSi-n with the spectrum of metallic Co. The similarities are clearer if we obtain the transform the spectra to the real space by obtaining the Radial Distribution Function (RDF, Figure 5c). In this figure the spacial distribution of neighbours around the scattered element is represented and gives an overall situation of the short range environment of the Co. In Figure 5c the similarities of CoPSi-n with metallic Co are clearer. In case of CoPSi-p, EXAFS spectra has more common features with CoO than with  $\text{Co}_3\text{O}_4$ : position and shape of the RDF in the first neighbour matches with the O in the CoO, but the second one matches with the position of Co atoms in the metallic Co, confirming the observations in XANES spectrum.

The elemental concentration profile of these systems is studied by Rutherford Back Scattering (RBS). RBS spectra and elemental profiles of both systems are depicted in Figure 6. Figure 6a,b, show the raw RBS spectra of the CoPSi-n and CoPSi-p samples, respectively, and the simulated spectra with the SIMNRA software [11]. A reference of Ta-Ti alternated multilayers was used to perform the energy calibration of the experimental system. By using this reference, a fine adjustment of the set up parameters was achieved. In the analyzed PSi systems, the porosity degree does not contribute significantly to the measured oxygen amount. The void (or porous) part of the samples does not produce backscattering nor energy loss, and a porous material is indistinguishable of a bulk one by this technique. This is a reason to not be able to determine porosity profiles directly by RBS. In this respect, other authors have carried out these calculations by filling pores with hydrocarbon solvents like pentane to obtain porosity profiles in PSi multilayers [17,18]. In these cases the filling substance can be quantified and an indirect measurement of the porosity can be obtained.

From the raw spectra (Figure 6a,b) we observe a clear difference in the profiles. The feature in the higher energies region corresponding to the Co presents a localized

broad peak in case of Co-PSi-p and an extended region for Co-PSi-n. In a first approximation there should exist differences in the Co distribution along the layer in both configurations. Both spectra present the Si (1600–1700 keV) and O (~1000 keV) edges with subtle differences that require finer calculations. By using the fitting software it has been determined that in Co-PSi-n structures, Co is uniformly distributed along the multilayer, and the oxygen concentrates mainly near the surface. This means that metallic Co is hosted in deeper zones of the multilayer and  $\text{Co}_3\text{O}_4$  is concentrated in outer zones of the matrix. For Co-PSi-p systems, Co penetrates to less deep zones and the O concentration keeps fairly constant along the multilayer. This is due both to the presence of O bubbles inside the matrix and the coexistence of a mixture of Co oxides. Figure 6c,d summarize the elemental in-depth profiles of each systems, CoPSi-n and CoPSi-p, respectively, obtained from the simulations of the experimental spectra.

A typical cross section of a CoPSi-n system is observed by TEM to study the distribution of the Co deposits along the PSi structure. A representative image is presented in Figure 7. In this image, the distribution of the Co NPs inside the PSi matrix can be clearly identified and also the porous structure of the PSi layer. An image in the STEM mode (inset to Figure 7), which enhances the contrast with the differences in atomic weight, facilitates the identification of Co inside the Si matrix. Again, Co NPs of circa 5 nm and spherical shape are observed

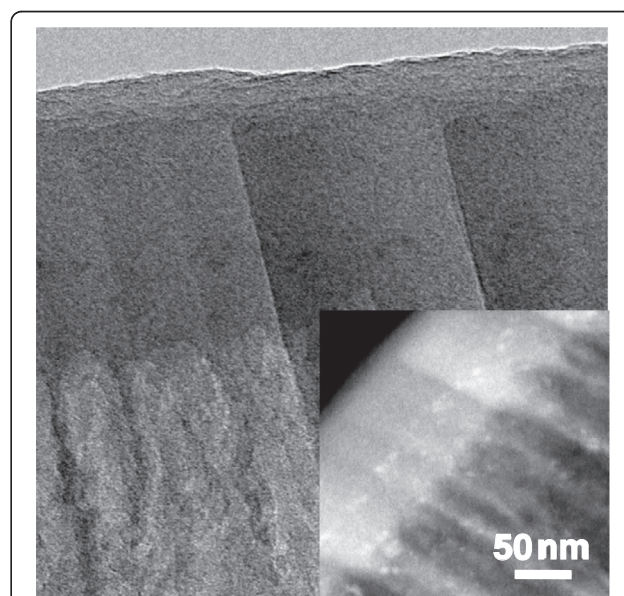


**Figure 7** Cross section TEM images of a sample Co-PSi-n showing the Co NPs inside the porous matrix. The inset is a magnification in STEM mode highlighting the atomic weight of the elements.

inside the PSi matrix, with a roughly uniform distribution of them inside the porous structure.

## Conclusions

In this work the protective effect of the matrix on the oxidation of electroinfiltrated Co nanoparticles into PSi has been proved. Moreover, a selected multilayer configuration in the matrix allows minimizing the formation of Co oxides that forms an oxidation profile in the whole layer depending on the porosity gradient of the PSi template. The magnetic properties of such Co-PSi systems suggest the possibility to control the magnetization of these hybrid materials by controlling the amount of infiltrated Co. Nevertheless, the influence of the PSi porosity type and degree in the oxidation of the hosted Co need to be further characterized. Future work in this sense should be performed in order to identify the physico-chemical properties of the PSi matrix that minimizes the oxidation in such hybrid materials.

## Acknowledgements

We acknowledge the European Synchrotron Radiation Facility for provision of synchrotron radiation facilities and the MEC and Consejo Superior de Investigaciones Científicas for financial support (PE-2010 6 0E 013). We would like to thank the BM25-Spline staff for the technical support.

This work has been supported by MICINN through projects FIS-2008-06249, MAT2009-14578-C03-02, MAT2008-06858-C02-01, and MAT2008-06858-C02-02, as well as Comunidad de Madrid, project NANOBIOMAGNET (S2009/MAT-1726) and European project MAGNIFYCO (Contract NMP4-SL-2009-228622). Technical support from ICTS Centro Nacional de Microscopia Electrónica (UCM, Madrid) is gratefully acknowledged.

## Author details

<sup>1</sup>Departamento de Física Aplicada, Universidad Autónoma de Madrid, Cantoblanco, Madrid 28049, Spain. <sup>2</sup>Departamento de Electrocerámica, Instituto de Cerámica y Vidrio (ICV-CSIC), Cantoblanco, Madrid 28049, Spain. <sup>3</sup>IMDEA Nanociencia, Cantoblanco, Madrid 28049, Spain. <sup>4</sup>GTB, ETSIT Telecomunicaciones, Universidad Politécnica de Madrid, Madrid 28040, Spain. <sup>5</sup>Instituto de Ciencia de Materiales de Madrid (ICMM-CSIC), Cantoblanco, Madrid 28049, Spain. <sup>6</sup>Institute of Advanced Energy, Kyoto University, Uji, Kyoto 611-0011, Japan.

Received: 14 May 2012 Accepted: 14 August 2012

Published: 2 September 2012

## References

- Osaka T, Asahi T, Yokoshima T, Kawaji J: **Electroless-deposited soft magnetic underlayer on silicon disk substrate for double-layered perpendicular magnetic recording media.** *J Magn Magn Mat* 2005, **287**:292.
- Martín-Palma RJ, Lakhtakia A: *Nanotechnology: A Crash Course.* Bellingham: SPIE; 2010.
- Pankhurst A, Thanh NKT, Jones SK, Dobson J: **Progress in applications of magnetic nanoparticles in biomedicine.** *J Phys D: Appl Phys* 2009, **42**:224001.
- Halm S, Bacher G, Schuster E, Keune W, Sperl M, Puls J, Henneberger F: **Local spin manipulation in ferromagnet-semiconductor hybrids.** *Appl Phys Lett* 2007, **90**:051916.
- Muñoz-Noval A, Sanchez-Vaquero V, Torres-Costa V, Gallach D, Manso-Silván M, García-Ruiz JP, Hernando-Perez M, de Pablo PJ, Martín-Palma RJ: **Silicon-based hybrid luminescent/magnetic porous nanoparticles for biomedical applications.** *J Nanophotonics* 2011, **5**:051505-8.
- Granitzer P, Rumpf K, Pölt P, Reichmann A, Krenn H: **Self-assembled mesoporous silicon in the crossover between irregular and regular**

arrangement applicable for Ni filling. *Physica E (Amsterdam)* 2007, **38**(1-2):205.

- Bisi O, Ossicini S, Pavesi L: **Porous silicon: a quantum sponge structure for silicon based optoelectronics.** *Surf Sci Rep* 2000, **38**:1.
- Ogata YH, Kobayashi K, Motoyama M: **Electrochemical metal deposition on silicon.** *Current Opin in Solid State and Mater Scie* 2006, **10**:163.
- Silvan MM, Langlet M, Duart JMM, Herrero P: **Preparation of interfaces for TEM cross-section observation.** *Nucl Instrum & Methods in Phys Res Section B-Beam Interact with Mater and Atoms* 2007, **257**:623.
- Ravel B, Newville M: **Athena, artemis, hephaestus: data analysis for X-ray absorption spectroscopy using IFEFFIT.** *J of Sync Rad* 2005, **12**:537.
- Mayer M: **SIMNRA, a simulation program for the analysis of NRA, RBS and ERDA.** *AIP Conf Proc* 2008, **475**:541.
- Knobel M, Nunes WC, Socolovsky LM, De Biasi E, Vargas JM, Denardin JC: **Superparamagnetism and other magnetic features in granular materials: a review on ideal and real systems.** *J Nanosci Nanotech* 2008, **8**:2836.
- Coe JMD: *Magnetism and Magnetic Materials.* Cambridge: Cambridge University Press; 2010.
- Corrias A, Mountjoy G, Loche D, Puentes V, Falqui A, Zanella M, Parak WJ, Casula MF: **Identifying spinel phases in nearly monodisperse iron oxide colloidal nanocrystal.** *J Phys Chem C* 2009, **113**:18667.
- Corrias A, Ennas G, Mountjoy G, Paschina G: **An X-ray absorption spectroscopy study of the FeK edge in nanosized maghemite and in Fe<sub>2</sub>O<sub>3</sub>-SiO<sub>2</sub> nanocomposites.** *Phys Chem Chem Phys* 2000, **2**:1045.
- Fernández-García MP, Gorria P, Sevilla M, Fuertes AB, Grenèche JM, Blanco JA: **Onion-like nanoparticles with γ-Fe core surrounded by a α-Fe/Fe-oxide double shell.** *J Alloys Comp* 2011, **509**:S320.
- Pászti F, Szilágyi E: **Pore structure investigations in porous silicon by ion beam analytical methods.** *Vacuum* 1998, **50**:451.
- Torres-Costa V, Pászti F, Climent-Font A, Martín-Palma RJ, Martínez-Duart JM: **Porosity profile determination of porous silicon interference filters by RBS.** *Phys Stat Sol (C)* 2005, **2**:3208.

doi:10.1186/1556-276X-7-495

**Cite this article as:** Muñoz-Noval et al.: Characterization of hybrid cobalt-porous silicon systems: protective effect of the Matrix in the metal oxidation. *Nanoscale Research Letters* 2012 **7**:495.

**Submit your manuscript to a SpringerOpen® journal and benefit from:**

- Convenient online submission
- Rigorous peer review
- Immediate publication on acceptance
- Open access: articles freely available online
- High visibility within the field
- Retaining the copyright to your article

Submit your next manuscript at ► [springeropen.com](http://springeropen.com)